天体計測学特論 I
Observational Astronomy I

Lecture 09:
Advanced technology
for optical/IR observations
adaptive optics / interferometer
discussions

Polarimetry : imaging / spectroscopy

Wollaston prism

Images are from Thorlabs inc. web page

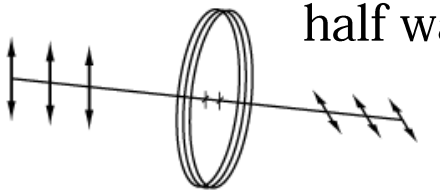

half wave plate

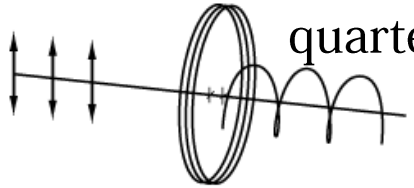

quarter wave plate

- Linear polarization :
  - half wave plate + Wollaston prism + mask
  - Take images at 0deg, 45deg, 22.5deg, 67.5deg.
- Circular polarization :
  - quarter wave plate + Wollaston prism + mask
  - Take images at 45deg, 135deg.

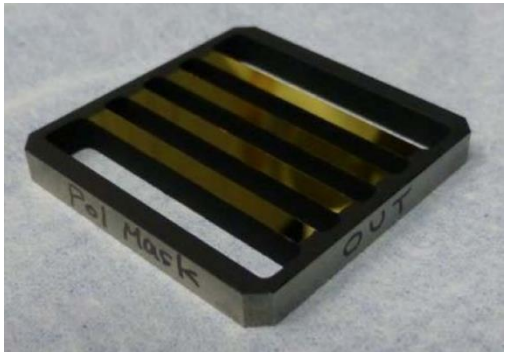

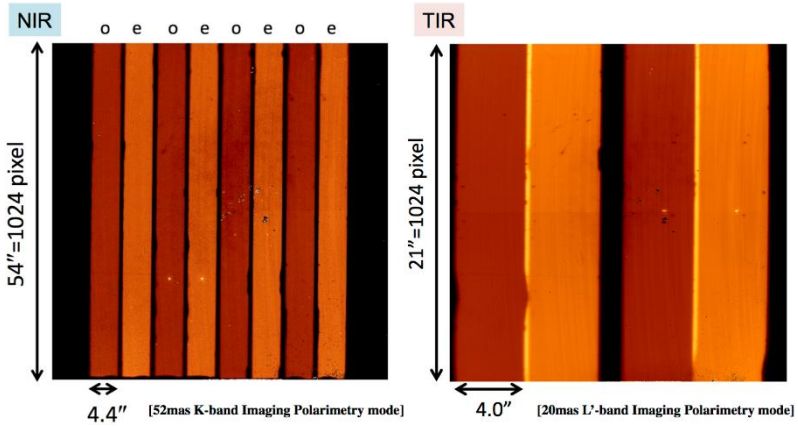

from Subaru/IRCS web page

- Generally, polarization degree is not high, if you want to measure polarization degree with 0.1% accuracy, you need to achieve SN~1000.

Polarimetric Differential Imaging

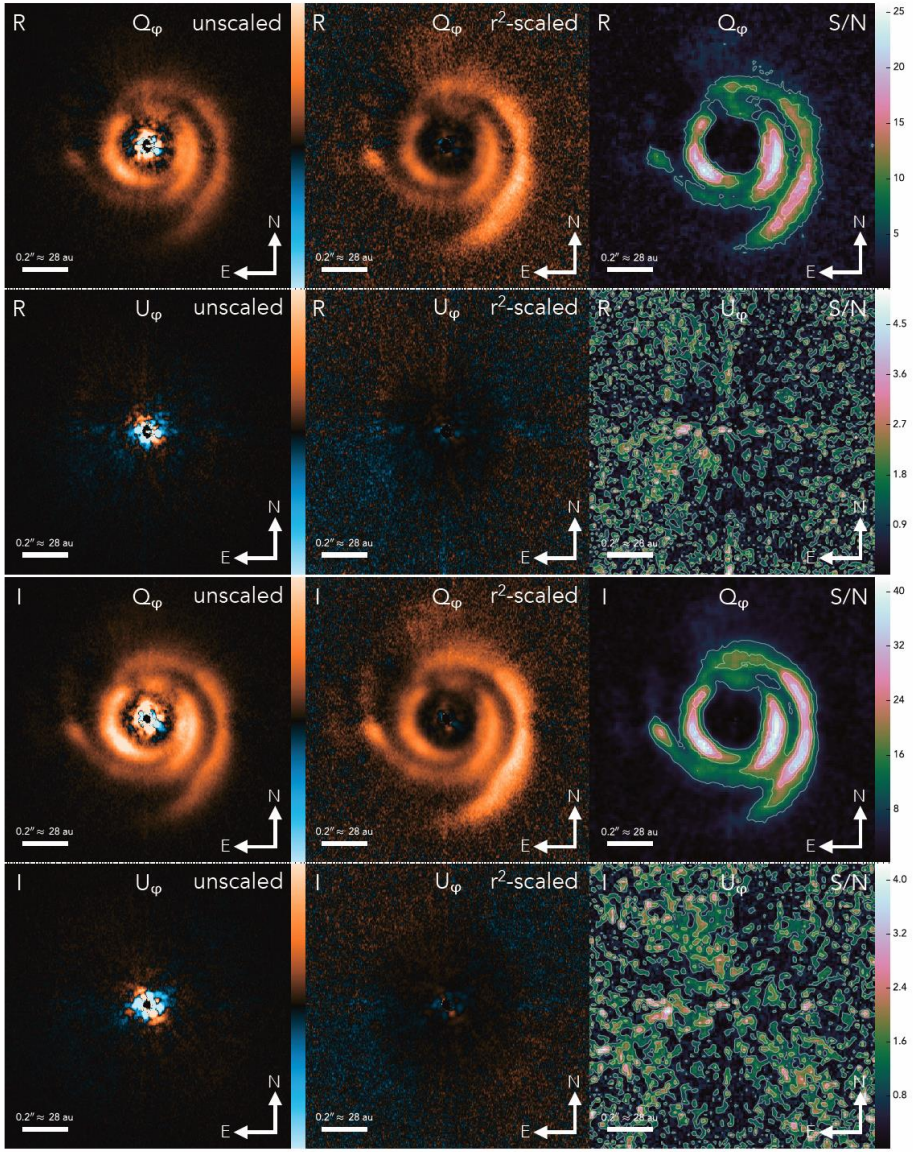

Fig. 1. ZIMPOL *R*-band (*top two rows*) and ZIMPOL *I*-band (*bottom two rows*) polarized intensity images. The field of view is 1.″4 × 1.″4 and the central star is positioned in the center of each image. The *left column* shows the Q_ϕ and U_ϕ polarized intensity images (see Sect. 2.3). The *center column* shows the Q_ϕ and U_ϕ images scaled with the deprojected distance squared from the star to each pixel for an inclination of 11° and a position angle of the major axis of 62°. All images are shown on a linear color stretch, with companion Q_ϕ and U_ϕ images having the same minimum and maximum value. Orange corresponds to positive values, blue to negative values, and black is the zero point. The *right column* shows the signal-to-noise (S/N) maps of the Q_ϕ and U_ϕ images which are obtained from the U_ϕ images. The contour levels correspond to the standard deviation values that are shown on the right of the S/N map colorbar.

- Scattered light is polarized.
- Scattered light can be detected in the polarimetry.

- Proto-planetary disk is illuminated by the central star, and we see the disk in the scattered light (in visible/NIR).

- Figure from Stolker et al. 2016

$$Q_\phi = Q\cos 2\phi + U\sin 2\phi$$
$$U_\phi = Q\sin 2\phi - U\cos 2\phi,$$

- Qphi>0 : azimuthal
- Qphi<0 : radial
- Uphi : 45deg tilted against Q

What can we see with very high spatial resolution ?

0.01” (TMT diff. limit @ 1.6um, Subaru diff. limit @ 0.4um)

- @ 1kpc => 10AU = 5x10^-5pc
  - Globular Cluster　M3:10kpc　M4:2kpc
  - M15:10kpc　(<500Ms, 15km/s) RBH~10^-3pc
- @ 8.5kpc => 85AU = 4x10^-4pc
  - Stars in the Galactic center region : smallest orbit r=0.05”=0.002pc=400AU
  - Proper motion 0.02”/yr=160AU/yr
  - Black hole at the MW center 3x10^6Ms Rs=0.06AU
  - Black hole radius of influence RBH~GM./sigma^2~0.03pc
- @ 1Mpc => 0.05pc
  - M31@720kpc, G1(M.=2x10^4Ms, sigma=30km/s) RBH~0.008pc
  - M33(M.<1000Ms, sigma=30km/s) RBH~4x10^-4pc…
- @ 20Mpc => 1pc
  - NGC1068@14.4Mpc
  - M87@18Mpc, Black hole mass and radius of influence 3x10^9Ms RBH~3pc
  - HST/FOS [OII] 0.1”=10pc resolution で観測されている。
- @ z=0.5 => 0.07kpc
  - A fewx10^10Ms　RBH~7pc。
- @ z=1.0 => 0.09kpc
- @ z=2.5 => 0.09kpc
- @ z=5.0 => 0.07kpc

Schematics for Natural / Laser Guide Star AO systems

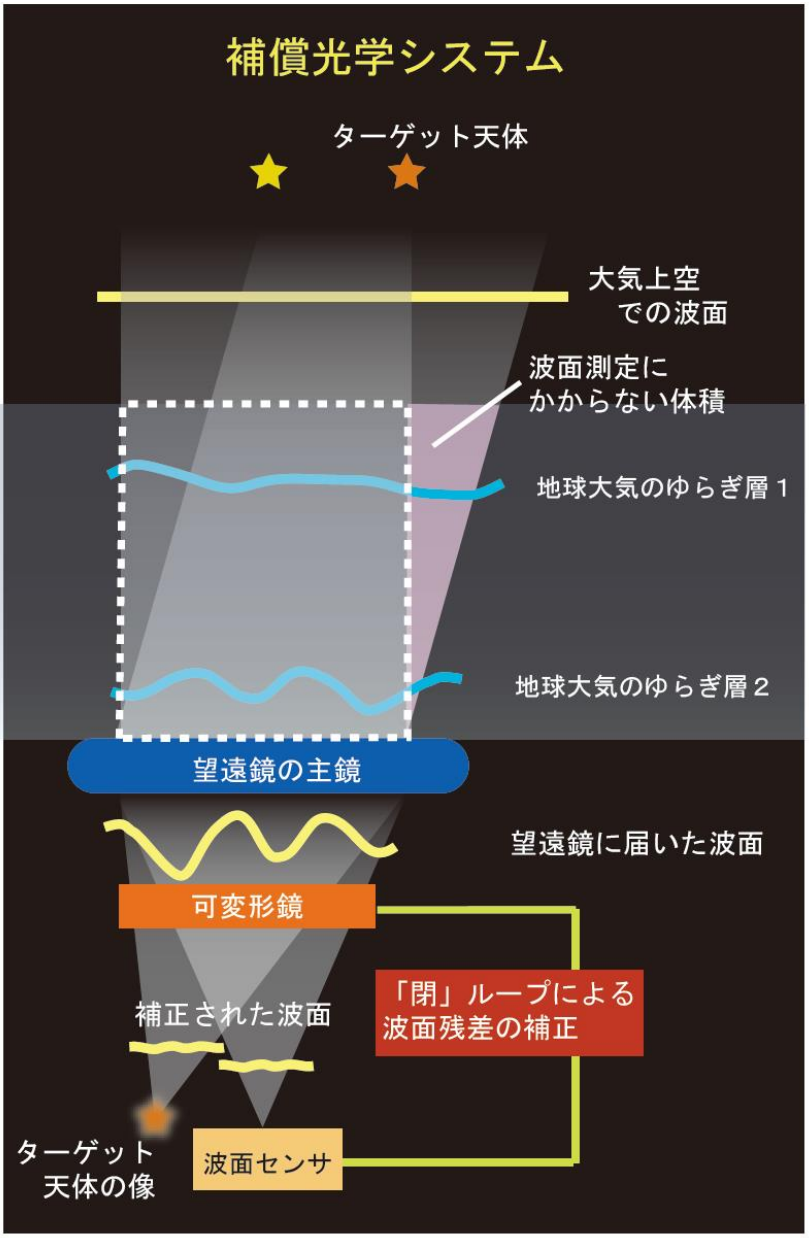

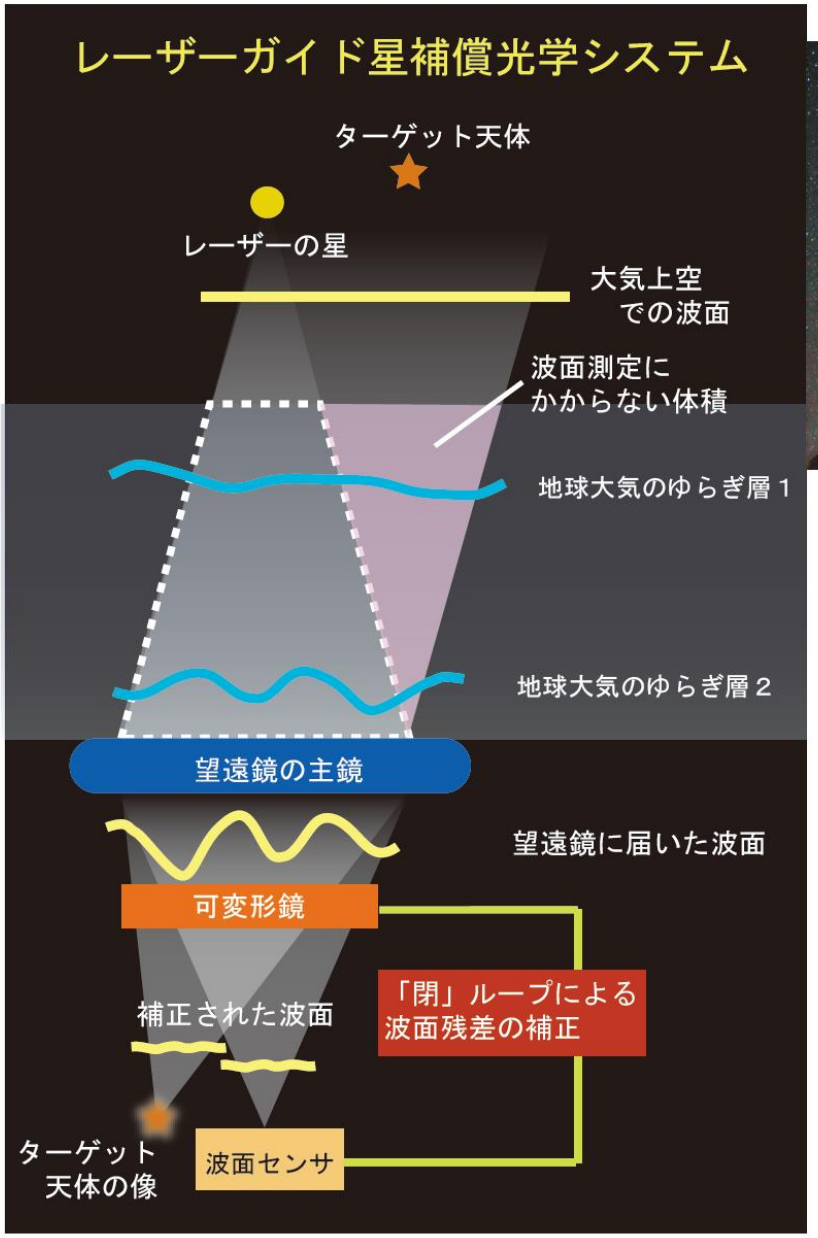

Laser Guide Star on sky

www.gemini.edu

Measuring atmospheric turbulence with Shack-Hartmann wavefront sensor

Reference spots with plane wavefront

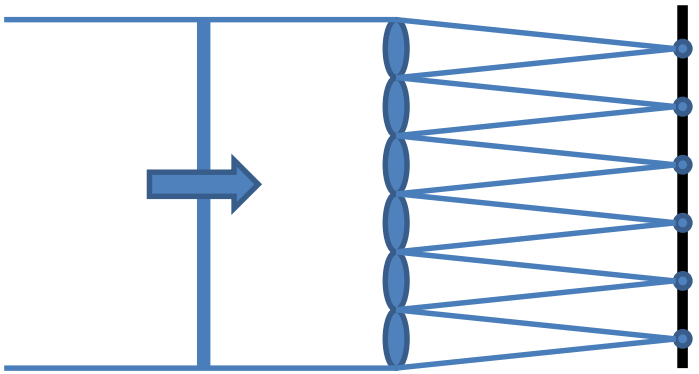

Distorted wavefront measured with the SH WFS

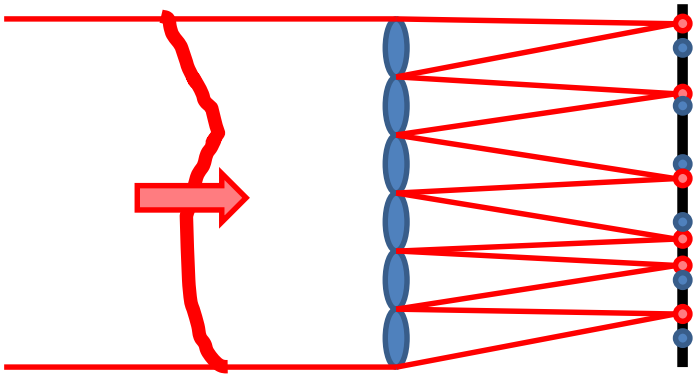

Reconstruction

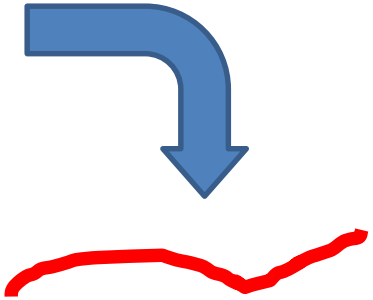

Real measurements with Shack-Hartmann wavefront sensor

– Sirius observed with 50cm telescope at the top of this buiding. 20 frames / sec.

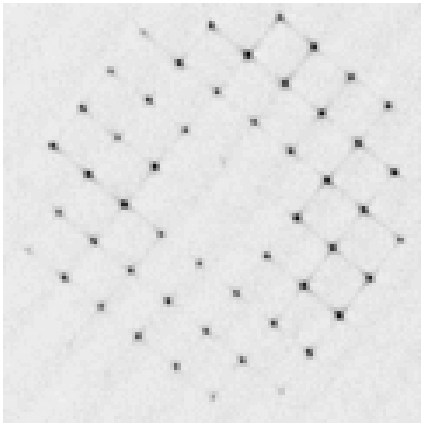

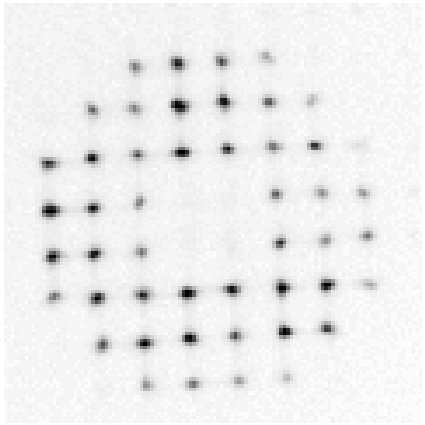

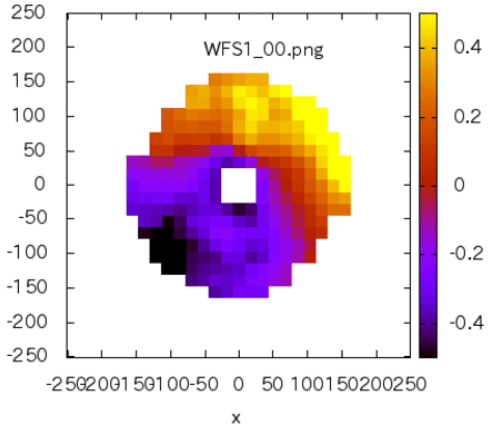

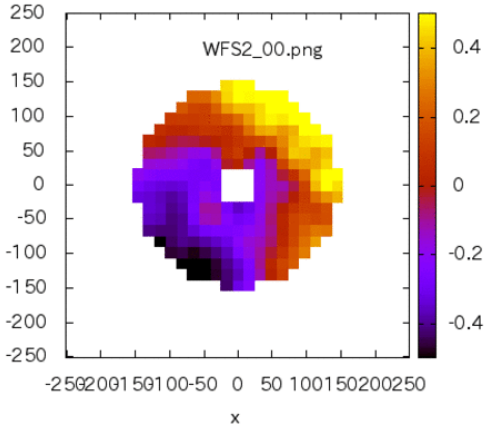

Simulation of a TMT adaptive optics observation

– Simulated Adaptive Optics system on TMT

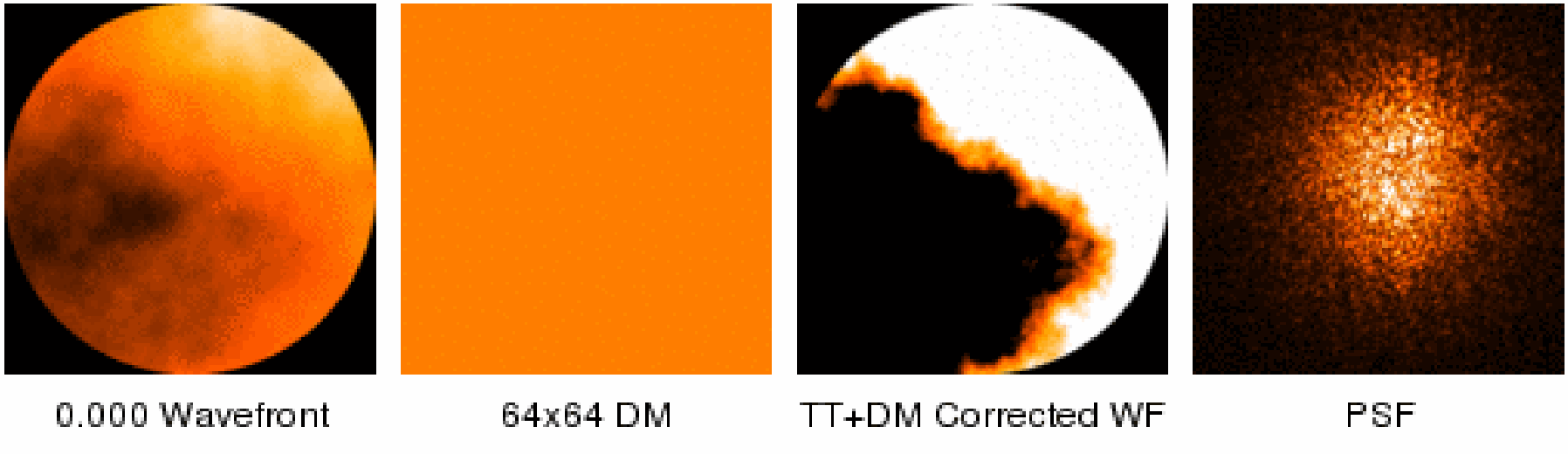

Measuring the movement of stars in the Galactic center

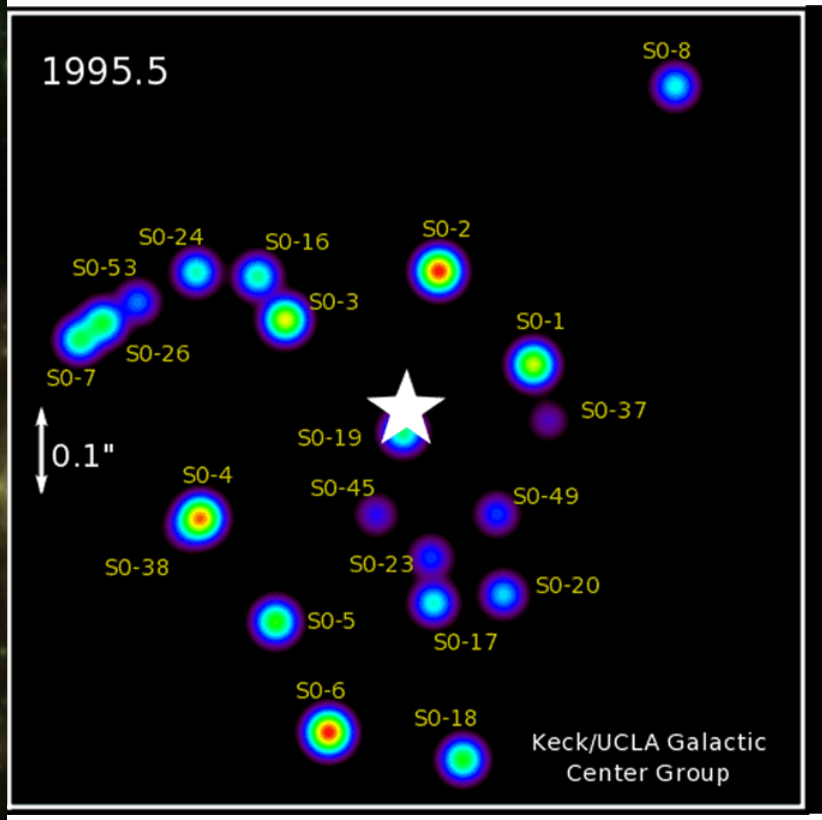

From http://www.astro.ucla.edu/~ghezgroup/gc/pictures/index.shtml These images/animations were created by Prof. Andrea Ghez and her research team at UCLA and are from data sets obtained with the W. M. Keck Telescopes.

Strehl ratio vs. Point Spread Function

– EE represents Ensquared Energy within 0.12″x0.12″, EE2 represents Ensquared Energy within 0.24″x0.24″. The squares in the top-left panel shows the squares.

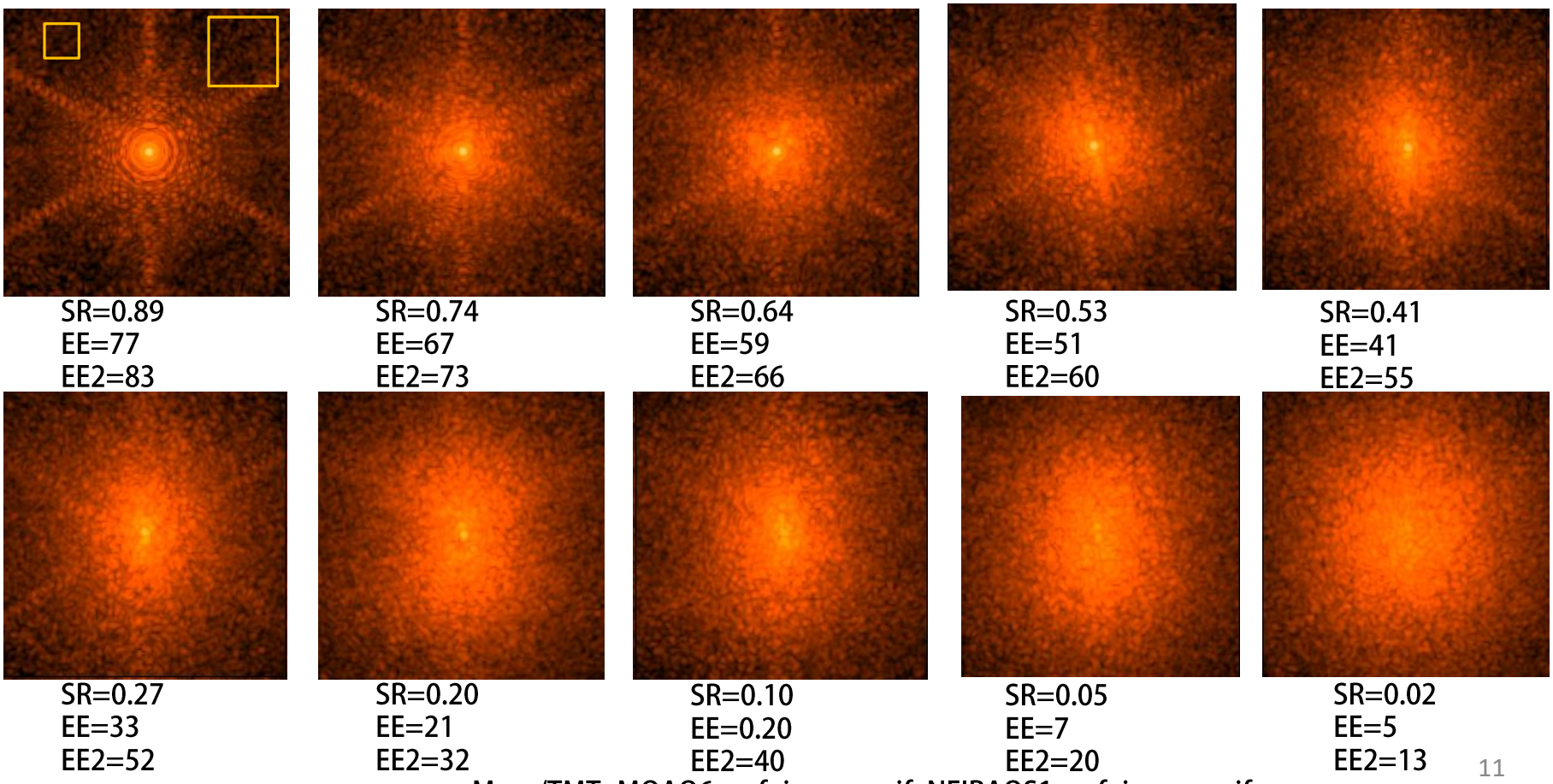

Maos/TMT_MOAO6_psf_images.gif, NFIRAOS1_psf_images.gif

Performance of AO system : number of elements

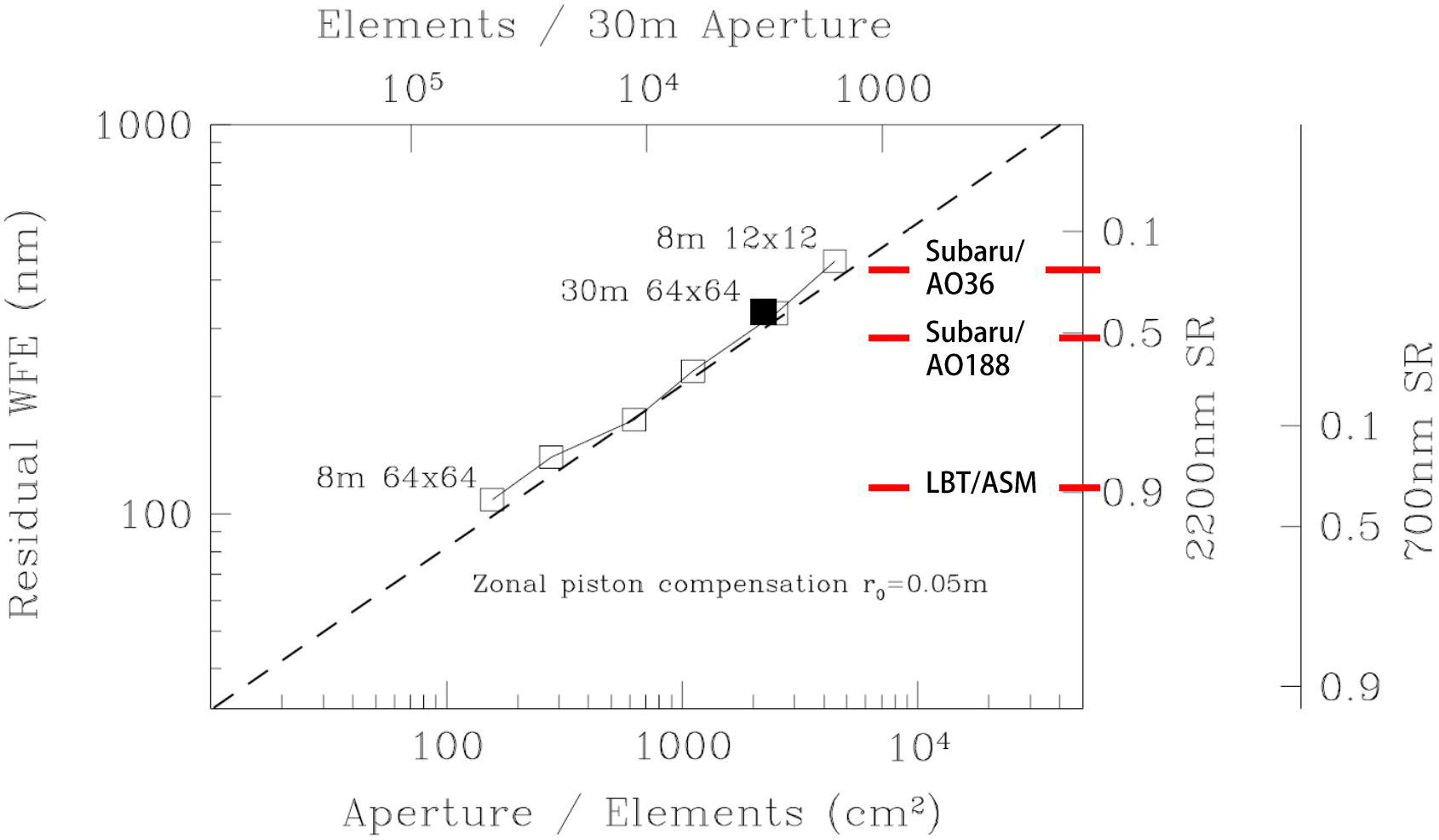

AOinst/SIMAO/number_rms.pdf

A simple coronagraph

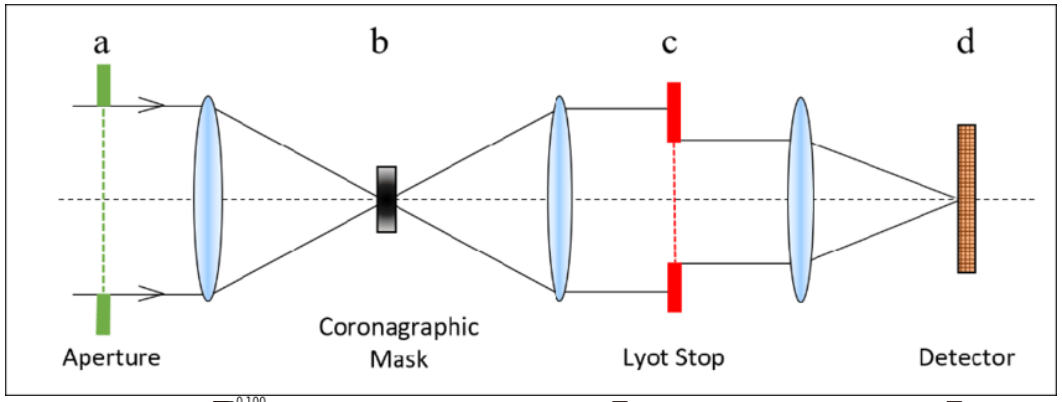

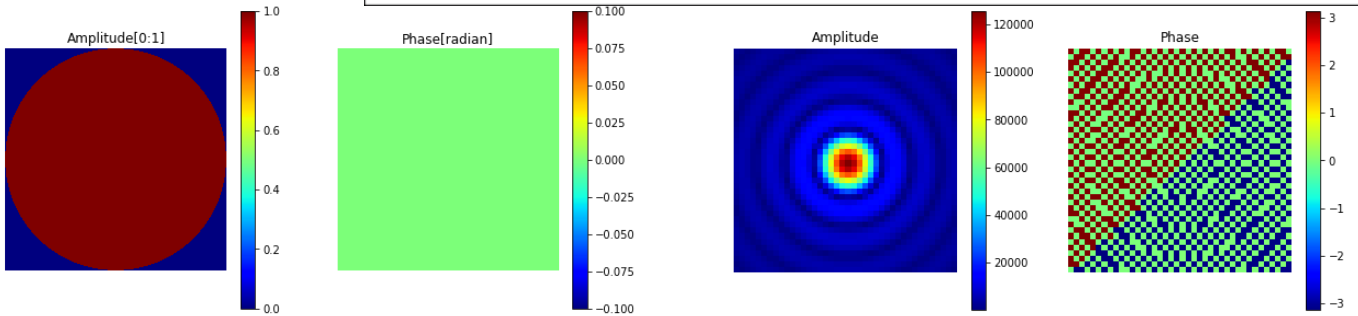

Amp^2 is the observed image

Apply CM

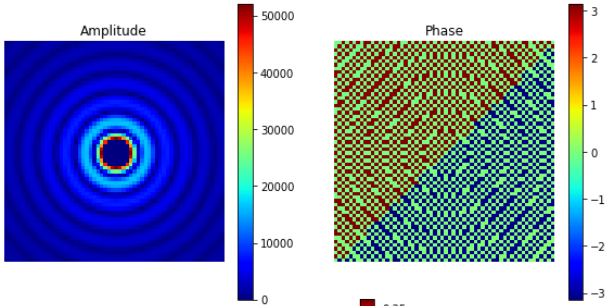

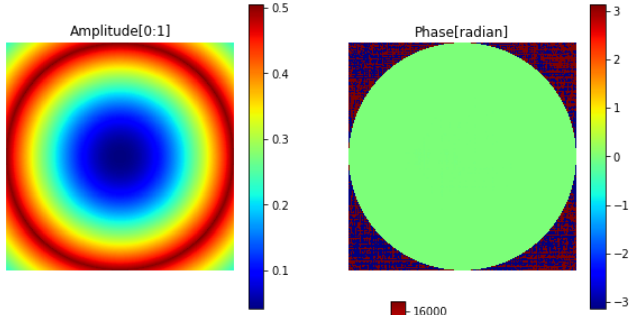

Apply LS

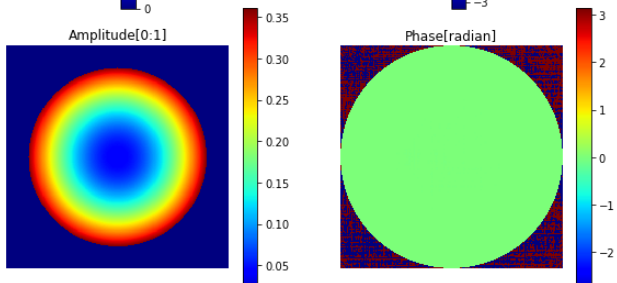

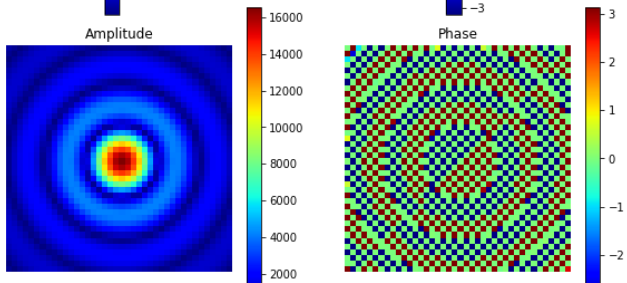

A design for the JWST coronagraphs

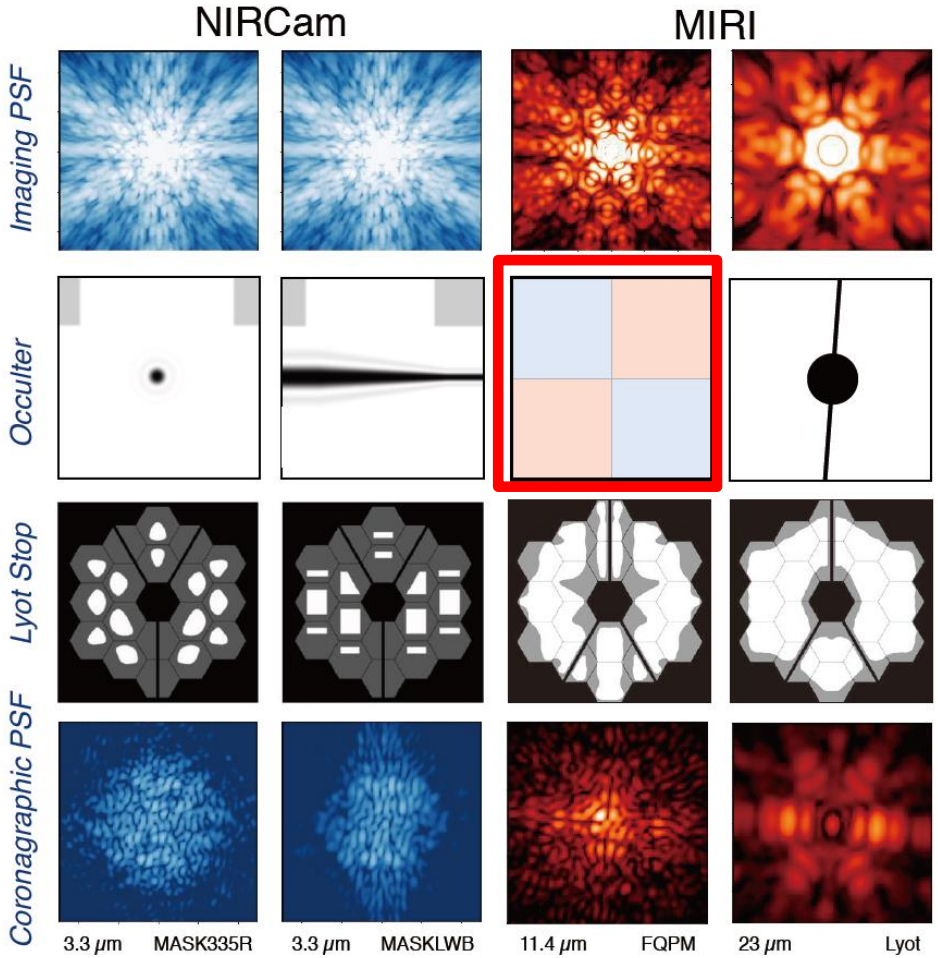

Figure 1: Schematic of representative coronagraph modes available on JWST with the NIRCam and MIRI instruments. The imaging and coronagraphic PSFs are shown with different logarithmic color stretches given their very different brightness levels. NIRCam includes 5 band-limited Lyot coronagraphs (3 circular and 2 bar masks, usable with a wide variety of filters). MIRI includes 3 four-quadrant phase masks and a classical Lyot coronagraph, each of which has a single dedicated spectral filter. The leftmost example, the NIRCam round mask at 3.3 μm, is used as the primary example mode for subsequent contrast plots.

Perrin et al. 2018, SPIE 10698-09

Interferometer

- Combine x4 8m telescope to form an interferometer.

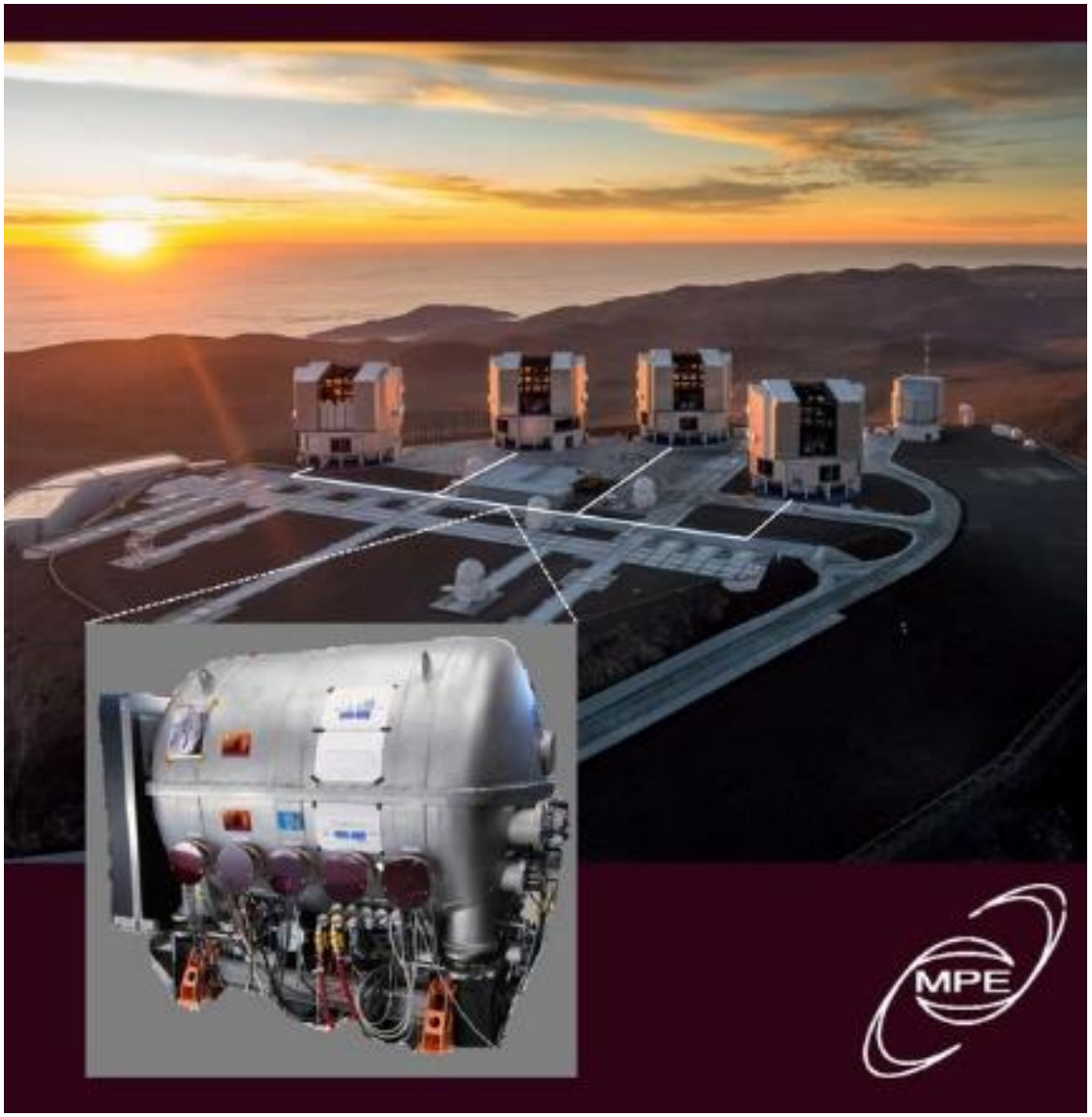

Interferometer

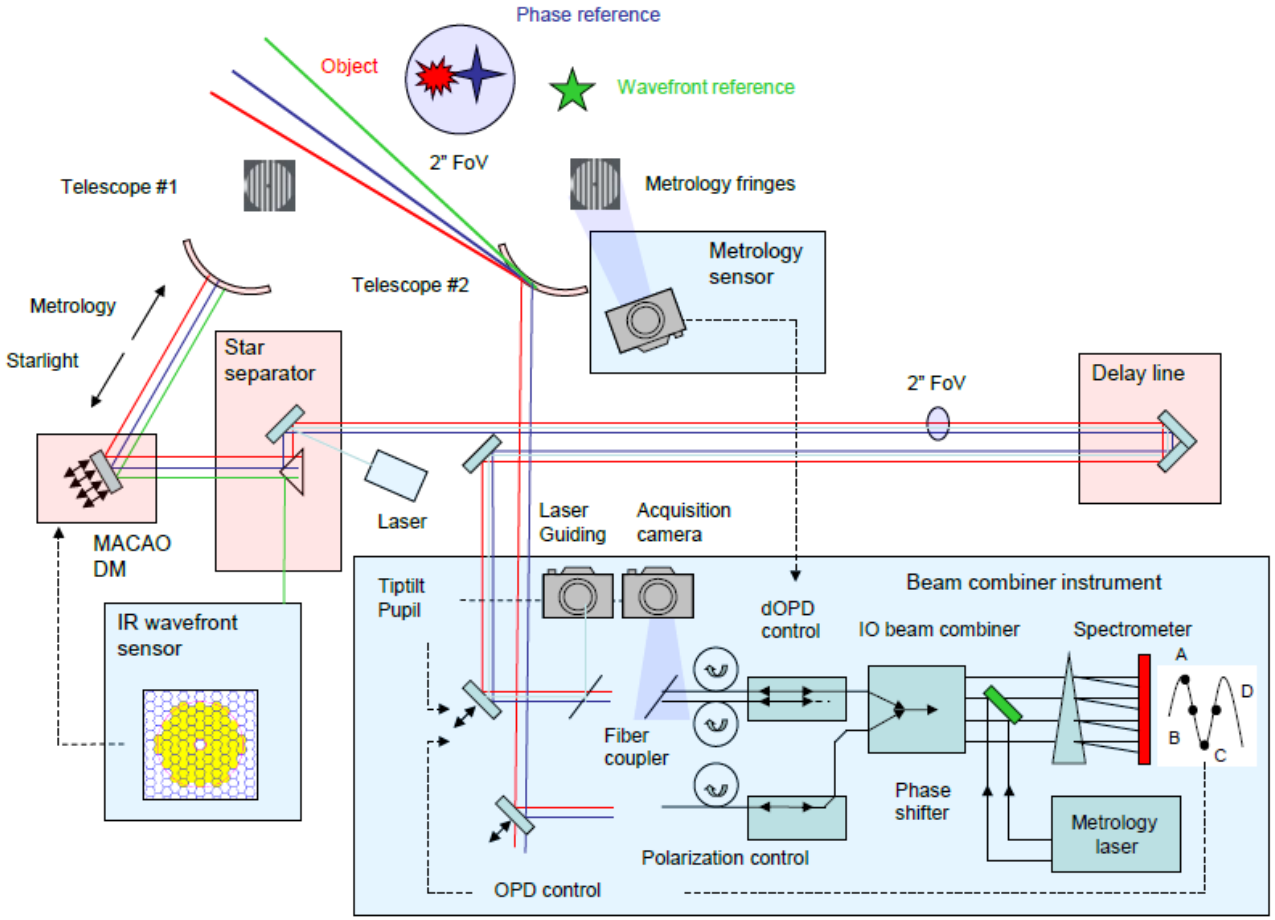

Fig. 1. Overview and working principle of GRAVITY: the instrument coherently combines the light of the four 8m UTs of the VLTI or the four 1.8m ATs. It provides infrared wavefront sensing to control the telescope adaptive optics, two interferometric beam combiners - one for fringe-tracking and one for the science object -, an acquisition camera and various laser guiding systems for beam stabilization, and a dedicated laser metrology to trace the optical path length differences for narrow angle astrometry. The overview illustrates the light path and location of the various subsystems. For clarity, we show only two telescopes, one beam combiner and one wavefront sensor. The wavefront sensor star (green) can be outside the VLTI field of view. Depending on the brightness of the science object (red), the fringe tracker is either fed by a beam splitter, or - as illustrated in this figure - by a bright off-axis phase reference star (blue). The GRAVITY subsystems (light blue boxes) are embedded and take advantage of the already existing VLTI infrastructure (light red boxes).

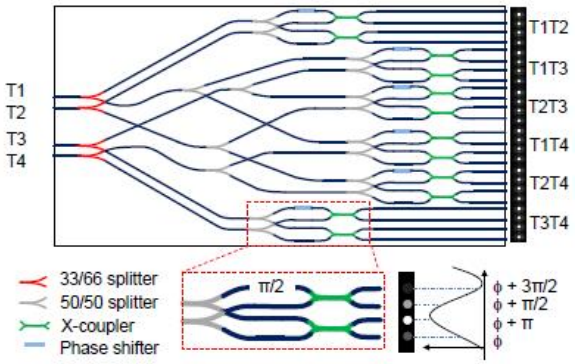

Fig. 5. Integrated optics beam combiner: the actual interference happens in an etched silica-on-silicon integrated optics chip. The top panel shows a photograph of the GRAVITY integrated optics, the lower panel the design of the circuit. The integrated optics contains all functions (dark blue: waveguides, red and gray: beam splitter, light blue: phase shifter, green: X coupler) for a pairwise combination of the four telescopes and fringe sampling. The light from the four telescopes T1 ... T4 is fed by single-mode fibers from the left, the output on the right is the interference of the six telescope combinations for a relative phase shift of 0°, 90°, 180°, and 270°, respectively.

- GRAVITY collaboration 2017

Galactic center with the interferometer

- NACO: AO, SINFONI:AO-IFU, GRAVITY:VLT interferometer.
- SINFONI : R~1,500
- GRAVITY : 5min x 34 integrations for March 2018

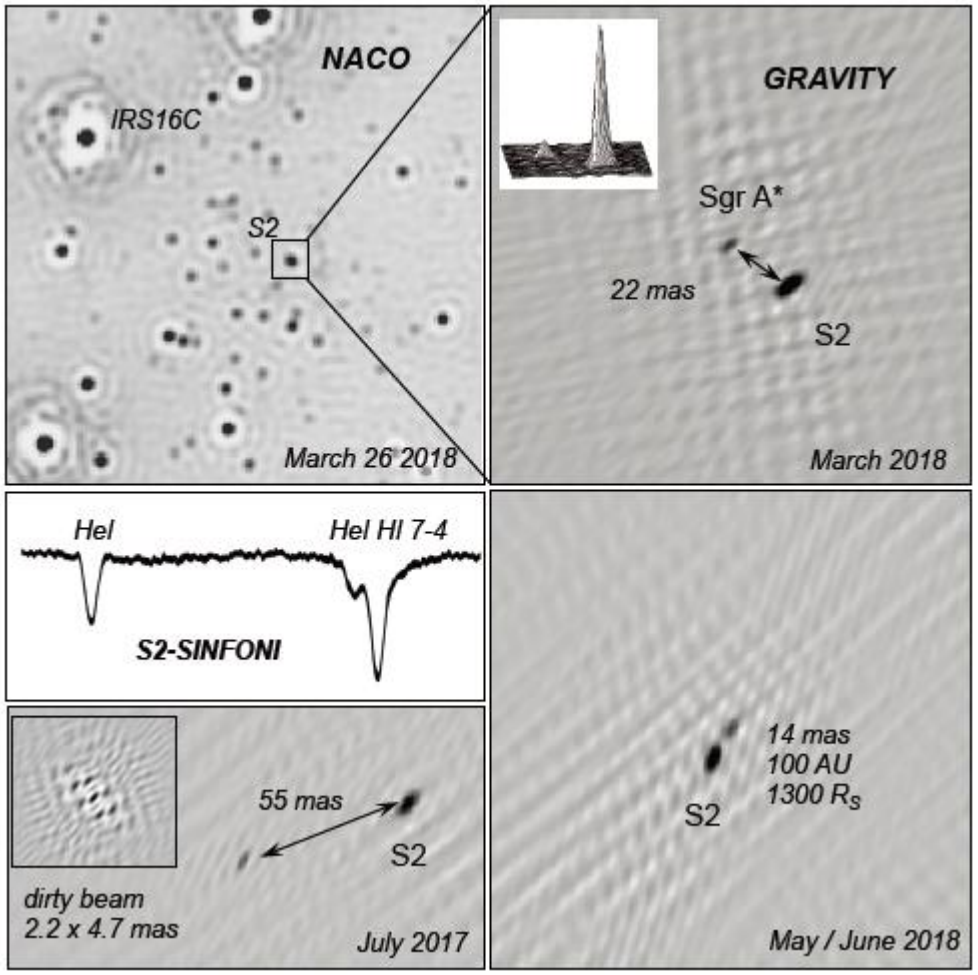

Fig. 1. Monitoring the S2 orbit around Sgr A* with the three VLT(I) instruments NACO (AO-assisted, single UT imaging), GRAVITY (interferometric astrometry-imaging with all four UTs of the VLT) and SINFONI (AO-assisted integral field spectroscopy). Upper left: Deconvolved NACO K-band image of the Galactic centre a few weeks before the 2018 pericentre passage. The source S2 appears slightly elongated because of confusion with Sgr A*. Upper right: Nearly simultaneous GRAVITY image of S2 and Sgr A*. The image shows the central 150 mas (0.0059 pc $\approx 1.4 \times 10^4\, R_S$) after self-calibration and CLEANing with AIPS. The image is reconstructed from 34 integrations of 5 minutes each from several nights at the end of March 2018. Sgr A* was (on average) $K = 16.6$ mag and the rms noise level of the background after cleaning is ≈ 20 mag. Both Sgr A* and S2 are unresolved. Here and in the other GRAVITY images, the elongation is due to the shape of the interferometric clean beam. Bottom: S2 - Sgr A* GRAVITY images (co-addition of several days) from July 2017 (bottom left) and May/June 2018, a few days after pericentre (bottom right). The inset in the bottom left panel shows the instantaneous interferometric beam, which is 2.2 mas × 4.7 mas without Earth rotation. The inset in the middle left shows a co-added SINFONI K-band spectrum of the star S2, taken from Habibi et al. (2017).

Active Galactic Nuclei with the interferometer

- 20 micro arcsec structure resolved with the interferometer.

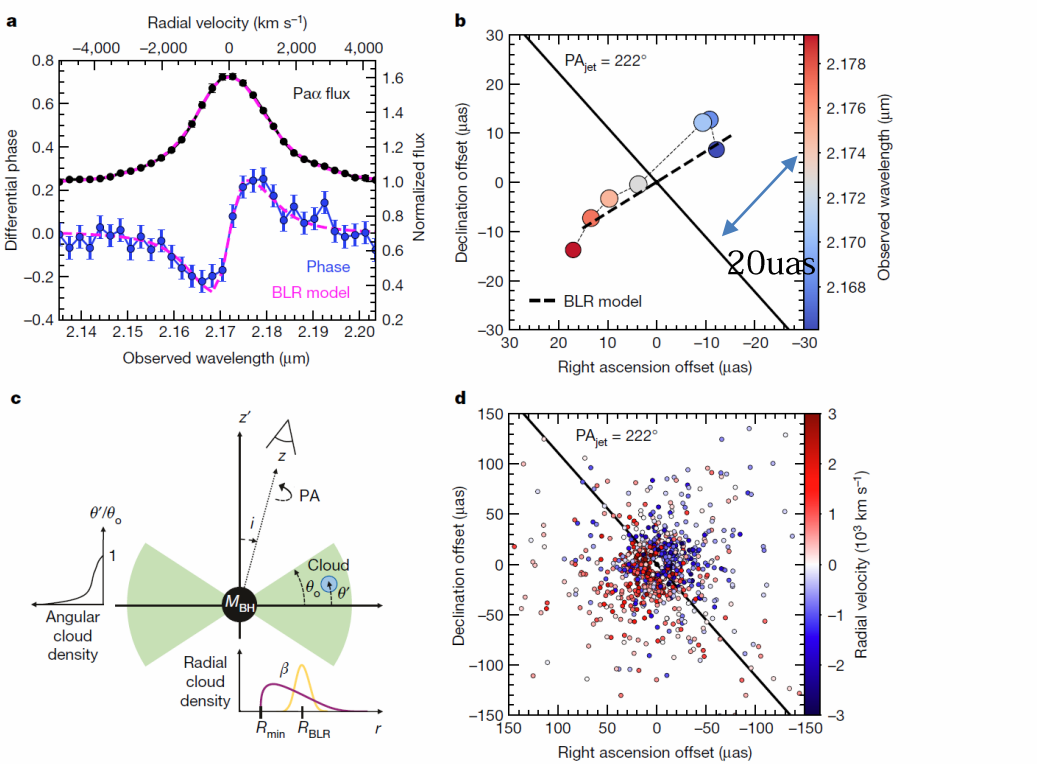

Fig. 1 | Main observational and modelling results. a, Paα line profile (black points; right axis) of 3C 273 observed by GRAVITY, along with the differential phase averaged over three baselines (blue points; left axis), showing the 'S' shape that is typical for a velocity gradient. The error bars represent 1σ. A thick-disk model of the BLR (dashed pink lines, see also **c** and **d**) provides an excellent joint fit to the data. **b**, The observed centroid position of the photo-centre in several wavelength channels (indicated by the colour scale; symbol size is proportional to the signal-to-noise ratio) show a clear spatial separation between redshifted and blueshifted emission: a velocity gradient at a position angle (PA) nearly perpendicular to that of the radio jet (PA_{jet}; solid black line). The centroid track of the BLR model is shown as a dashed line. **c**, Schematic representation of the model parameters. The green shaded area shows the geometry of the gas that surrounds the supermassive black hole (of mass M_{BH}), with the blue circle indicating an individual gas cloud. The angular (θ'; normalized by the opening angle of the disk θ_o) and radial (r) distributions of the gas clouds are plotted on the left and below, respectively. The rotation axis of the disk points along z', which is inclined by an angle i to the line of sight z. **d**, Velocity map (colour scale) of the model that best fits the discrete clouds (points)—a thick disk geometry viewed nearly face-on. Disorder in the velocity map reduces the observed shifts in the photo-centre (**b**) compared to the angular size of the BLR (**d**).